Comparative Study of Dynamical Requirement Impacts on System Design of Notional Aircraft Dc and Ac Electric Power Systems

Le Kong
Center for Ultra-Wide-Area Resilient Electric Energy Transmission Networks (CURENT)
The University of Tennessee, Knoxville
TN, USA
lkong4@vols.utk.edu

Fei (Fred) Wang
Center for Ultra-Wide-Area Resilient Electric Energy Transmission Networks (CURENT)
The University of Tennessee, Knoxville
Oak Ridge National Lab
TN, USA
fred.wang@utk.edu

***Abstract*— In future aircraft electric power systems (EPSs), the dc distribution is regarded as a promising substitution for conventional ac distribution because of the reduced weight. However, the assessment of weight reduction is usually obtained under the system static performance requirements. Dynamical requirements, including small-signal stability, normal load transient, and abnormal transient have not been fully considered. Therefore, this paper aims at bridging this gap by providing a design example under comprehensive system requirements to study the impacts of dynamical requirements on dc and ac, separately. It is seen that if only static requirements are considered, dc EPS is lighter than ac mainly due to the lighter feeders. But if dynamical requirements are factored in, the notional dc EPS will need additional energy storage systems (ESS) and protection devices because it lacks energy storage capability and has faster fault current dynamics intrinsically, comparing with the notional ac EPS.**

Keywords*— *aircraft electric power system, ac system, dc system, dynamical requirement, stability

I. Introduction

In most conventional electric power systems, ac is the dominant power type. But with the development of power-electronics converters, more and more applications tend to adopt dc power due to the improved efficiency, controllability, cost, and size. Examples include data center, dc residential power system, MVDC shipboard system, and high-voltage transmission lines, etc. [1-4]. Among these trending dc applications, aircraft electric power system (EPS) is one of the most popular topics as reported in [5-10].

A chart regarding the historical evolution of electric power and voltage of on-board EPSs is shown in Fig. 1 [8]. In the first days of powered flight, the aircraft EPSs (6 V /12 V dc voltage and less than 500 W) were mainly designed for communication and ignition systems. Then, with the installation of lighting, signaling, and heating systems, the dc voltage level was increased to 28 V, and the generator capacity was increased up to 1 kW. In the 1960s and thereafter, with the increased electric power demand due to the increasing speed and size of aircraft, integration of ac generation was observed, due to its several advantages comparing with dc generations [8, 9]. First, the power density of ac generations (0.66 - 1.33 kVA/kg) was higher than dc topology (less than 0.5 kW/kg) in the 1950s. Second, a potentially much higher voltage, i.e., 115 Vac comparing with 28 Vdc, could be adopted which would bring a cabling weight reduction. Third, there was no need for commutators in ac generators, therefore, the system reliability was improved. In addition, 400 Hz was selected among many candidates (60, 180, 240, 360, 400, and 800 Hz) as the standard frequency by the Army Air Corps in 1943, and then made mandatory for use by the US Air Force in 1959, since it was more feasible for the generator speed with practically minimal motor and transformer weight. However, to obtain the constant frequency, constant speed drives (CSD) were needed which required regular maintenance and increased weight and size of the system. In addition, the onboard energy-consuming loads, i.e., resistive loads, are frequency insensitive. While for the frequency-sensitive loads, by connecting transformers and/or more mature power electronics converters with the variable frequency generators, certain voltage types can be achieved easily. For these reasons, from the 1980s and onwards, the main bus voltage of aircraft EPSs uses a hybrid system with 115 Vac and a variable frequency of 360 - 800 Hz. Starting from the 1990s, the major thrust for the evolution of aircraft EPSs is the reduction of fuel consumption for an eco-friendly system and a possible weight reduction, which promotes the more electric aircraft (MEA) concept, e.g., Boeing B787 and Airbus A380. That is, all the aircraft secondary systems which are currently operated by mechanical, hydraulic, and pneumatic systems will be replaced by electric systems. Due to the increasing power demand, the main bus voltage is also increased in some newer developments using 230 Vac with variable frequency or 270/540 Vdc. But the optimal solution to using ac or dc for the main bus voltage is still under investigation for the future MEA and electrified propulsion.

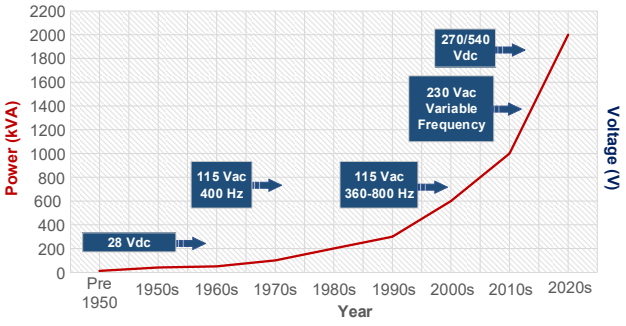

Fig. 1. Electric power and voltage evolutions of aircraft EPSs.

To fully capture the pros and cons of using ac power and dc power, comparative studies are usually conducted. This comparative study of ac and dc aircraft EPSs are similar to other trending dc applications in the literature [11-16], e.g., microgrids or high voltage transmission lines, with a different design goal, i.e., the minimum system weight. However, the existing comparisons have been mainly conducted under the

system static requirements (e.g., power balance, total harmonic distortions, thermal limits, etc.), while the impacts of dynamical requirements on system design have not been considered. Therefore, this paper aims to develop a design process to study the impacts of the dynamical requirements on system design. Notional dc and ac EPSs are designed under both static requirements and dynamical requirements. Besides, system weight as the design target is used to quantify the dynamic impacts.

II. Notional Structure and Design Requirements of Aircraft EPSs

An example architecture of MEA EPS is shown in Fig. 2 based on the EPS of the B787. There are four variable frequency starter/generators, four 540 Vdc 18-pulse autotransformer rectifier units (ATRU), four 28 Vdc 18-pulse transformer rectifier units (TRU), two 6-phase inverters, and many protection devices [17].

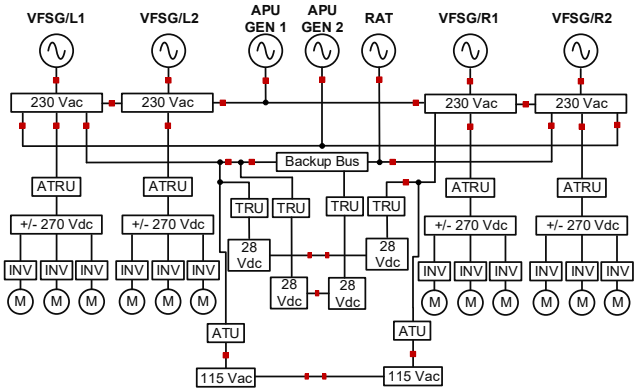

Fig. 2. Example architecture of an MEA EPS.

From this example, it can be seen that the main components of an aircraft EPS include generators, rectifiers, motor loads, and resistive loads. Another example of a 20 MW electrified aircraft in [6] also has a similar structure and components. Therefore, to simplify the design process, and meanwhile, to keep the intrinsic characteristics of aircraft EPSs, the system is simplified as two notional structures as shown in Fig. 3.

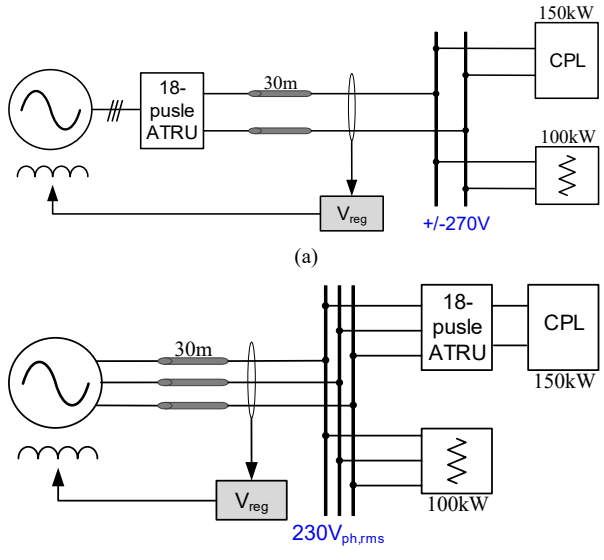

Fig. 3. Notional aircraft EPSs.

The main bus voltages of the two notional systems are +/- 270 Vdc and 230 Vac, respectively. Also, in each system, it is assumed that there are one 150 kW inverter-driven motor load which is modeled as a constant power load (CPL), and one 100 kW resistive load. The feeder length in both systems is assumed to be 30 m. The source side is a synchronous generator (SG). And an 18-pulse ATRU is used to convert ac voltage to dc voltage in both systems. Additionally, no redundancy for system safety is considered in this study.

In addition to the given notional structure and working conditions, the desired system performance and a design goal should also be clarified to kick off the design procedure. In this paper, the performance requirements for both ac and dc notional systems are from the following aircraft EPS standards: SAE-AS-50881F, MIL-STD-704E, and RTCA/DO-160G. And the design goal for the aircraft EPS is to minimize the weight of the aircraft electric system. Therefore, with the given system framework, loading conditions, performance requirements, and certain objectives, a conceptual design of these two notional aircraft EPSs can then be conducted.

III. Conceptual Design of Aircraft EPSs Considering Static Requirements

The conventional sizing methods of aircraft EPS include (1) framework and component models to determine power demands, (2) power distribution for insulated conductors (insulation thickness and insulation materials), (3) wiring, and (4) heat exchanger design [18, 19]. This study is mainly focused on the electric component design, including the sizing of cables, ATRUs, and generations.

To design the system under static requirements, several assumptions are made first:

(a) Feeders are single insulated aluminum conductors (600V, 175ºC) with a 50mm spacing in-plane arrangement as shown in Fig. 4;

(b) The ambient temperature is assumed as -20 ºC when the aircraft flying altitude is 40,000 feet and +40 ºC when the aircraft is on the ground;

(c) Power factor and efficiency of 18-pulse ATRU in this paper are assumed to be 0.98 and 98% based on the current technology [20].

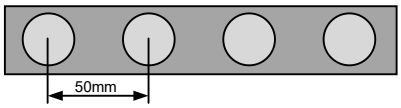

Fig. 4. In-plane arrangement of conductors.

With all the assumptions, the design procedure can then follow the weight determination algorithm as shown in Fig. 5. With the given load power and system losses, line currents can be obtained. Considering permissible temperature ratings, the cable diameter is chosen based on SAE-AS-50881F. Then, the result is checked with the bundle and altitude derating factors. If the current capability of the selected wire does not meet the line current requirements, then a larger cable diameter should be selected and examined. If it meets the requirements, then the generator power ratings can be calculated. The system weight can then be estimated according to the power density data.

Therefore, the feeders in ac EPS are selected to be 4×AWG 4/0 (47.85 kg) and in dc EPS are 2×AWG 2/0 (23.93 kg). Correspondingly, the required SG power ratings are obtained: the generator in ac system is 297 kVA and in dc

system is 291 kVA. Assuming the power density of the SG is 0.34 kg/kVA and of the ATRU is 0.24 kg/kVA, the weight of the SG and ATRU for both systems can then be calculated.

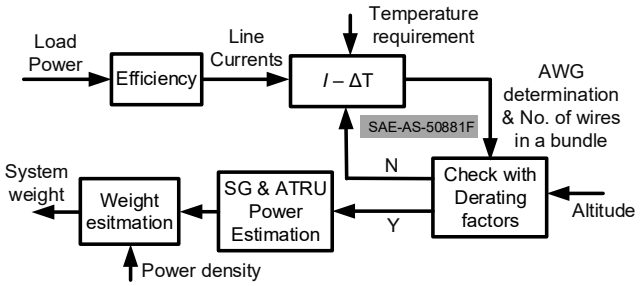

Fig. 5. System weight determination algorithm.

IV. Conceptual Design of Aircraft EPSs Considering Dynamical Requirements

The dynamic performance of aircraft EPS is also important for system design. Hence, impacts of dynamical requirements on system design are studied in this section, including small-signal stability, normal load transient, and abnormal transient.

A. Small-Signal Stability Design

Small-signal stability performance is examined with the static design results obtained in Section III.

1) Ac notional EPS

The passivity-based stability criterion is used for ac system analysis, i.e., if the bus impedance of the ac system is passive, then it is a stable system. In the ac system, the bus impedance can be modeled as the parallel connection of the input impedance seen from the ATRU side, the resistive load R_L, and the output impedance of the source side Z_{ov} as shown in Fig. 6.

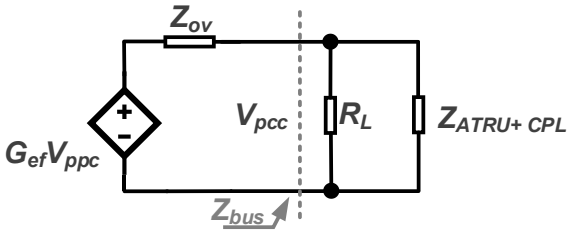

Fig. 6. Bus impedance of the ac notional EPS.

The SG is assumed as an ideal voltage source, so the passivity of the bus impedance is mainly determined by $Z_{ATRU+CPL}$. Modeling of the sequence impedance of the 18-pulses ATRU can be found in [21]. The small-signal stability criterion for the ac notional system is then simplified as (1).

$$Re\{Z_{ATRU}(j\omega)\} > 0, \forall\omega \in (-\infty, +\infty) \quad (1)$$

Therefore, the stability analysis can be conducted with the Bode diagram as shown in Fig. 7 and it is seen that the ac notional system is small-signal stable with the static design results. Note that the passivity-based criterion is a conservative approach. In this paper, the static design happens to result in a passive design, therefore, for simplicity, the passivity-based criterion can be used. But in other cases, if the bus impedance is not passive, it does not necessarily mean the system is unstable, and the Nyquist stability criterion should be adopted for further verification.

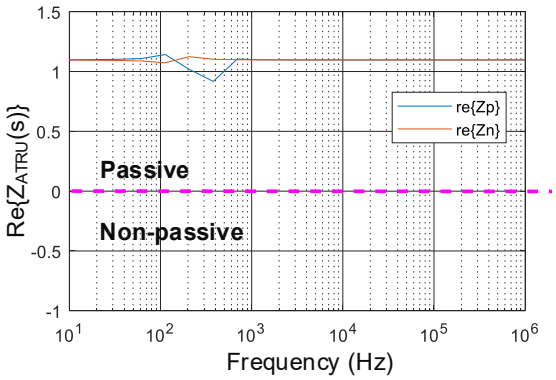

Fig. 7. Passivity-based stability analysis of the notional ac EPS.

2) Dc notional EPS

The Middlebrook criterion is used for the dc notional EPS to check the interaction of the impedances between the source side and load side as shown in Fig. 8. The generator and the 18-pulse ATRU are regarded as the source side and the output impedance is modeled as Z_S. The overall load side impedance is modeled as Z_L. Besides, the dc voltage control loop is denoted by T_v as shown in Fig. 8(b) with f_{BW} as its control bandwidth.

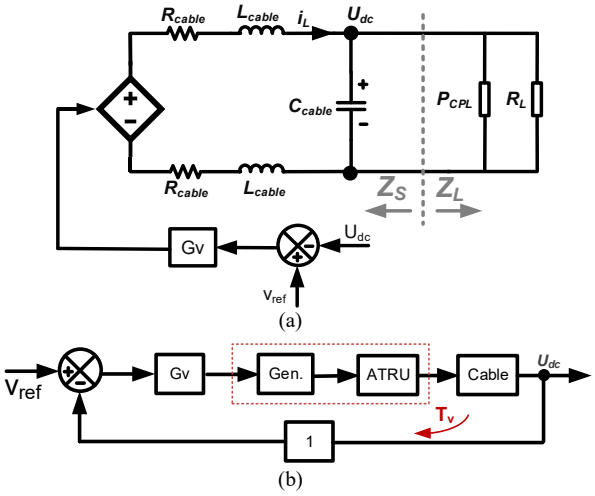

Fig. 8. Impedance models of the dc notional EPS.

The stability criterion for the dc notional system is given in (2), which shows that the stability margin Z_m of the system should be larger than 0 dB.

$$Z_m = 20log_{10}(|Z_L|) - 20log_{10}(|Z_s|_{peak}) \geq 0dB \quad (2)$$

where,

$$Z_L = \frac{-R_L V_{dc}^2}{P_{CPL}R_L - V_{dc}^2} \text{ and } |Z_s|_{peak} = \frac{1}{2\pi f_{BW} C_{cable}}$$

It is then calculated that the dc EPS is stable with a 32 dB impedance stability margin. Therefore, there is no need to modify the static design results. The Middlebrook criterion is also a conservative approach, so if the impedance ratio does not meet the stability requirement in (2), the Nyquist stability criterion is needed for further check.

B. Normal Load Transient Design

For normal load transient performance estimation, simulations with load step-down and step-up (100% to 5% to 100%) transients are conducted for both systems.

1) Ac notional EPS

The simulation results of load step-down transients are given in Fig. 9. As the load reference steps down from 100% to 5% of the overall power value, ac currents will follow a quasi-sinusoidal trajectory and drop to 0, and the ac contactor will switch at this zero-crossing point. Therefore, there is no large voltage spike.

During the load step-up transient, the response of ac bus voltage can also meet the standard as shown in Fig. 10. Therefore, there is no need to modify the original design for the ac system that is obtained under static requirements.

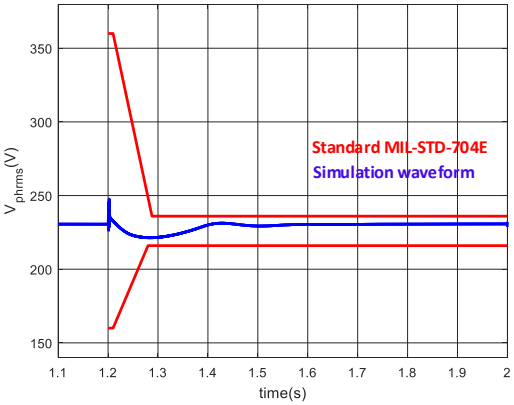

Fig. 9. Load step down in ac EPS from 100% to 5% at t = 1.2 s.

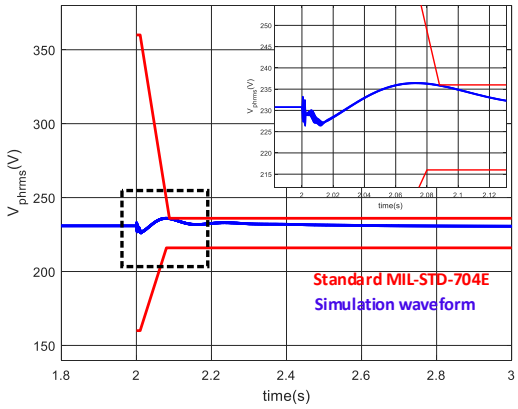

Fig. 10. Load step-up in ac EPS from 5% to 100% at t = 2 s.

2) Dc notional EPS

Similarly, the load transient simulations are conducted on the dc notional EPS as shown in Fig. 11 and Fig. 12. It is seen that the dc bus voltage during load step-down can meet the transient standard, but the load step-up transient cannot meet the requirement. Therefore, there is a need to modify the previous static design for the normal transient performance.

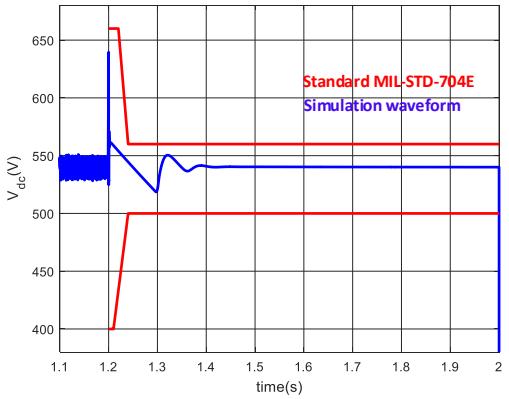

Fig. 11. Load step-down in dc EPS from 100% to 5% at t = 1.2 s.

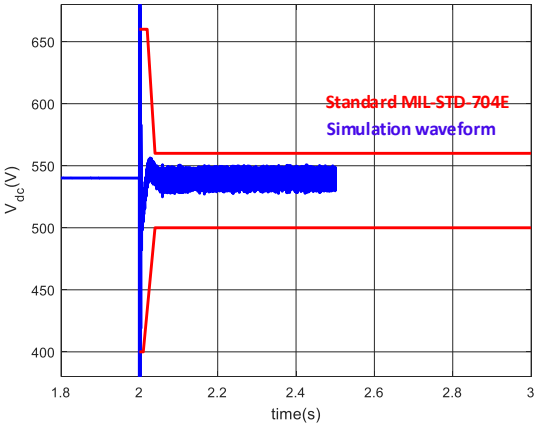

Fig. 12. Load step-up in dc EPS from 5% to 100% at t = 2 s.

The reason for this sharp voltage spike during load step-up transient in dc system is due to the lack of energy storage capability. Therefore, a dc-link capacitor is needed. The scheme of the modified dc system is shown in Fig. 13. And the transient bus current and voltage can be estimated by (3) and (4) so that the required dc-link capacitance can be calculated.

$$\frac{di_L}{dt} = -\frac{R_{cable}}{L_{cable}} i_L + \frac{V_{dc} - U_{dc}}{2L_{cable}} \tag{3}$$

$$\frac{dU_{dc}}{dt} = \frac{i_L}{(C_{cable} + C_{dcbus})} - \frac{P_{CPL}}{(C_{cable} + C_{dcbus})U_{dc}} - \frac{U_{dc}}{(C_{cable} + C_{dcbus})R_L} \tag{4}$$

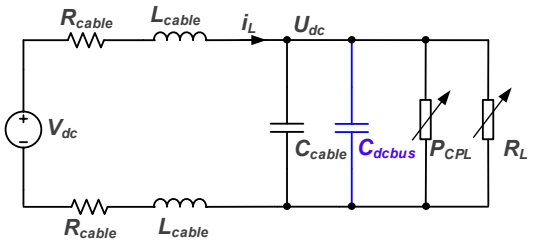

Fig. 13. Modified dc system considering load step-up transient.

In this study, a 5 mF (9kg) bus capacitor is required to meet the load transient requirements. The simulation results of the load transient with adding a bus capacitor are shown in Fig. 14 and Fig. 15.

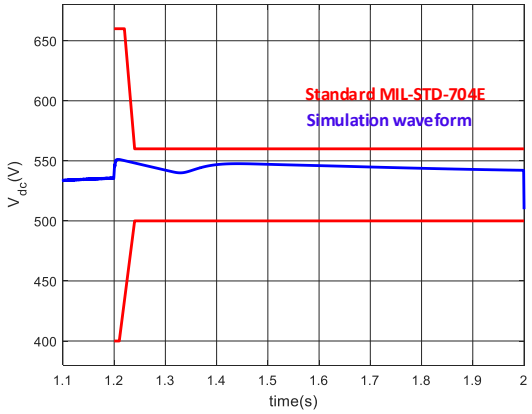

Fig. 14. Load step-down in dc EPS from 100% to 5% at t = 1.2 s.

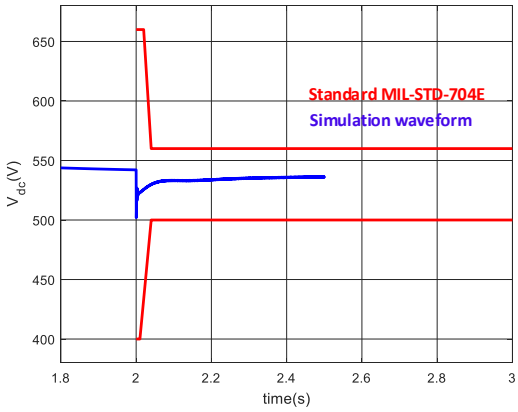

Fig. 15. Load step-up in dc EPS from 5% to 100% at t = 2 s.

It is shown that with the modified design, the normal load transient performance can meet the standard. In addition, the small-signal stability margin needs to be recalculated. In this case, the modified system was verified to be stable with a reduced stability margin, i.e., 6.3 dB.

C. *Abnormal Transient Design*

In addition to the normal load transient, the abnormal transient performance should also be considered. Therefore, for such a study, a phase-to-phase short-circuit fault and a pole-to-pole short-circuit fault is assumed separately in the ac and dc EPSs at the input side of the CPL with the short-circuit resistance R_{short} = 0.01 Ω at t = 1 s. The natural responses of the relative bus currents (= real current / nominal current) of both systems are given in Fig. 16 and Fig. 17.

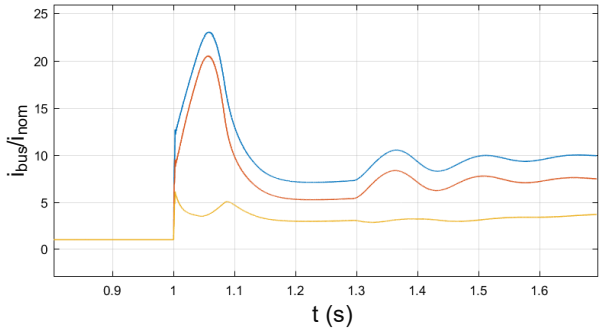

Fig. 16. Relative bus currents during a fault at t = 1 s in ac EPS.

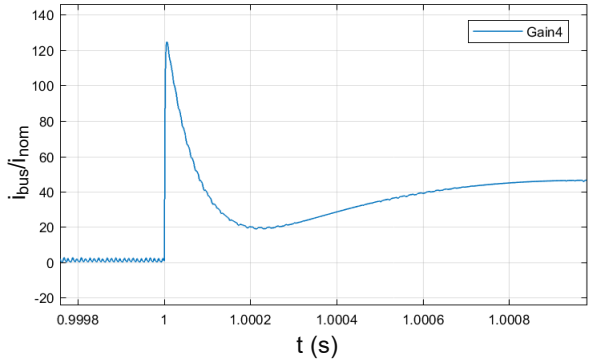

Fig. 17. Relative bus currents during a fault at t = 1 s in dc EPS.

It can be seen that the natural response of the fault currents in the dc EPS (×120 i_{nom}) is much larger than that in the ac EPS (× 23 i_{nom}). This is because the voltage holding capability of the dc bus capacitors is much larger than that in ac system as shown by the equivalent circuits of the immediate transient during fault of both systems in Fig. 18.

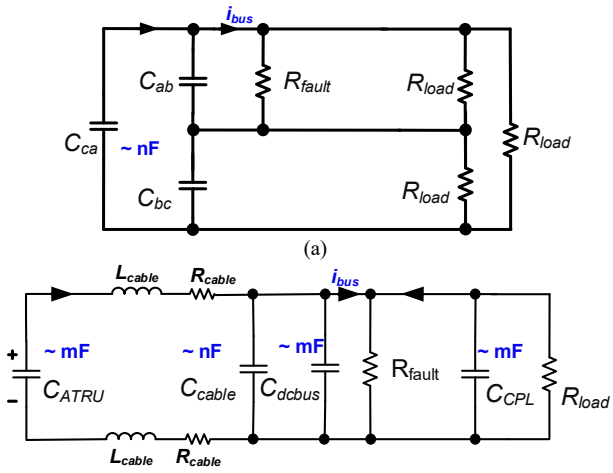

Fig. 18. Equivalent circuit of immediate transient: (a) ac EPS and (b) dc EPS.

To limit the fault current to be less than 9 times of the nominal current based on the requirements, the combined use of a superconducting fault current limiter (SFCL) [22], which is to suppress the fault current, and a solid-state circuit breaker (SSCB) [23], which is to quickly isolate faults, is assumed in this study. In addition, the response time of SSCBs used in this paper is assumed as 50 µs. The bus performance during faults with proper protection devices is shown in Fig. 19 and Fig. 20. Based on the simulations, it is found that the required equivalent resistance of SFCLs in the dc EPS is about two times of that in ac EPS. Therefore, the power ratings for the protection devices can be calculated. For faults at other locations or of other types, similar simulations are conducted and the corresponding protection devices can be selected. Note that the design of the protection devices is conducted under the complete selectivity conditions. In the end, with assuming the power density of the SSCBs (ac: 2.9 g/kW, dc: 5 g/kW) and the SFCLs (ac: 1.58 g/kW, dc: 0.524 g/kW), total weight of all the protection devices can then be estimated (ac: 16.9 kg, dc: 20.4 kg).

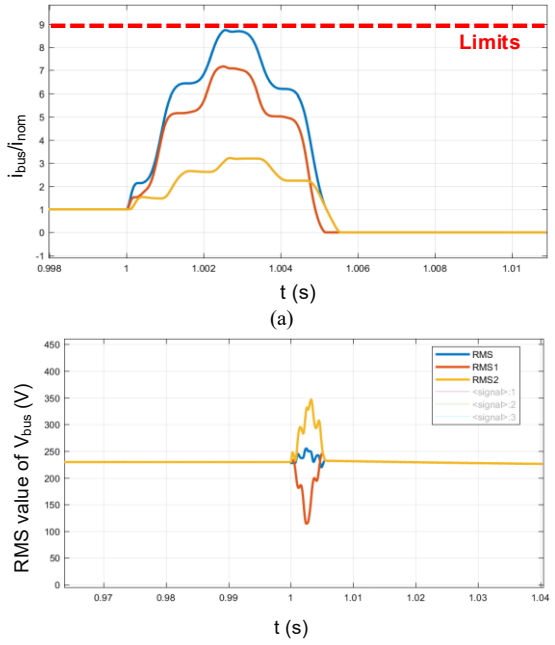

Fig. 19. Bus currents and voltage during a fault in ac EPS with protection devices: (a) relative bus currents and (b) bus voltage.

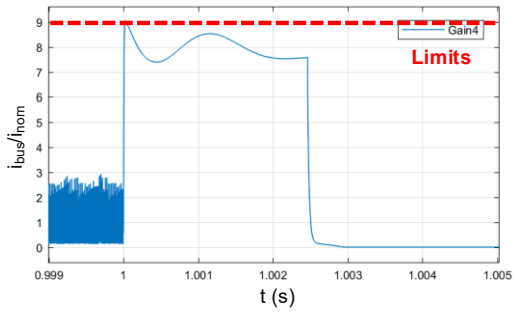

(a)

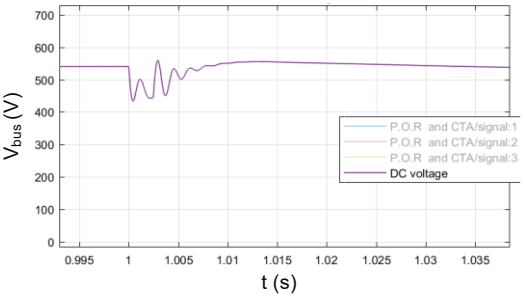

(b)

Fig. 20. Bus currents and voltage during a fault in dc EPS with protection devices: (a) relative bus currents and (b) bus voltage.

V. Design Results and Discussions

The overall system weight considering both static requirements and dynamic requirements can then be summarized as shown in Fig. 21, with the breakdown comparisons of each part in Fig. 21(a) and system weight comparisons with and without considering dynamical requirements in Fig. 21 (b).

From the results, it can be seen that compared with ac EPS, dc EPS saves some weight due to lighter feeders under static requirements only. But if the dynamical requirements are included, dc EPS will need an additional dc bus capacitor to provide energy storage capacity during the load transient. It also requires larger SFCL to limit the much faster fault current dynamics. Therefore, the weight reduction of using dc instead of ac would be much less significant due to the more impacts of dynamical requirements on dc than on ac.

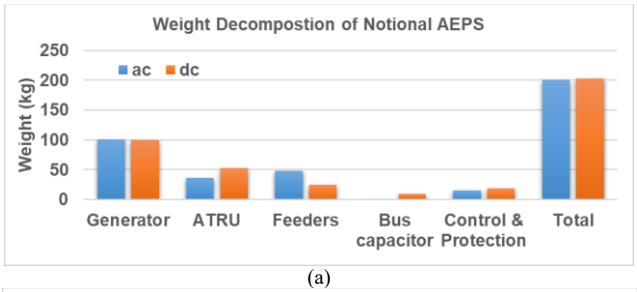

(a)

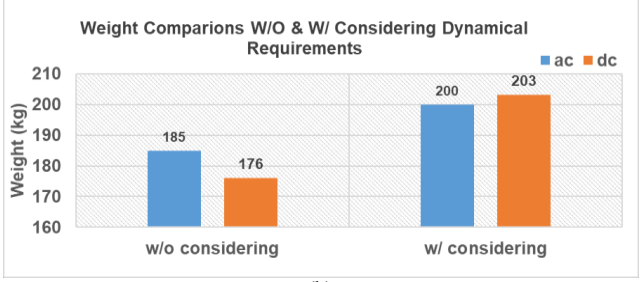

(b)

Fig. 21. Estimated system weight: (a) weight decomposition of notional Aircraft EPS and (b) weight comparisons.

Note that the power density values used in this study are from the literature or commercial products which might change with different technologies, but the methods to consider the impacts of dynamical requirements on system design are general.

VI. Conclusions and Future Work

This paper examined the impacts of dynamical requirements on the system design of dc and ac EPSs. If only static requirements are considered, the dc EPS will be lighter than ac EPS mainly because of the lighter feeders in the dc case. However, if dynamical requirements are considered as well, the dc EPS might be heavier than the ac EPS due to the need for extra ESS to provide enough short-term energy during load transient and larger SFCL to limit the faster fault currents. Therefore, dynamical requirements have more impact on dc system design than ac. The same methodology in the design process can also be extended to other applications with certain design goals, e.g., dc and ac microgrids design for minimized system cost.

For future work, the design of EMI filters and the groundings should be included. The design process considering system dynamical requirements introduced in this paper can also be extended to aircraft EPS with electrified propulsion. Also, system design under different voltage levels considering the dynamic impacts is interesting to be investigated.

Acknowledgment

This work was supported primarily by the Engineering Research Center Program of the National Science Foundation and the Department of Energy under NSF Award Number EEC-1041877 and the CURENT Industry Partnership Program.

References

[1] D. Boroyevich, I. Cvetković, D. Dong, R. Burgos, F. Wang, and F. Lee, "Future electronic power distribution systems a contemplative view," in *International Conference on Optimization of Electrical and Electronic Equipment*, 2010, pp. 1369-1380.

[2] W. Yang, Z. Yibin, Z. Donglai, and H. Han, "The technical trends and suggestions on the development of DC power grid," in *International Conference on Power System Technology*, 2014, pp. 1975-1979.

[3] E. Rodriguez-Diaz, M. Savaghebi, J. C. Vasquez, and J. M. Guerrero, "An overview of low voltage DC distribution systems for residential applications," in *IEEE International Conference on Consumer Electronics - Berlin (ICCE-Berlin)*, 2015, pp. 318-322.

[4] V. A. K. Prabhala, B. P. Baddipadiga, and M. Ferdowsi, "DC distribution systems-An overview," in *International Conference on Renewable Energy Research and Application (ICRERA)*, 2014, pp. 307-312.

[5] J. Brombach, T. Schröter, A. Lücken, and D. Schulz, "Optimized cabin power supply with a +/− 270 V DC grid on a modern aircraft," in *International Conference-Workshop Compatibility and Power Electronics (CPE)*, 2011, pp. 425-428.

[6] P. Kshirsagar *et al.*, "Anatomy of a 20 MW Electrified Aircraft: Metrics and Technology Drivers," in *AIAA/IEEE Electric Aircraft Technologies Symposium (EATS)*, 2020, pp. 1-9.

[7] B. Rahrovi and M. Ehsani, "A Review of the More Electric Aircraft Power Electronics," in *IEEE Texas Power and Energy Conference (TPEC)*, 2019, pp. 1-6.

[8] V. Madonna, P. Giangrande, and M. Galea, "Electrical Power Generation in Aircraft: Review, Challenges, and Opportunities," *IEEE Transactions on Transportation Electrification,* vol. 4, no. 3, pp. 646-659, 2018.

[9] A. K. Hyder, "A Century of Aerospace Electrical Power Technology," *Journal of Propulsion and Power,* vol. 19, no. 6, pp. 1155-1179, 2003.

[10] Z. Xin, J. M. Guerrero, and W. Xiaohua, "Review of aircraft electric power systems and architectures," in *IEEE International Energy*

Conference (ENERGYCON), 2014, pp. 949-953.
[11] R. W. Johnson. "AC versus DC power distribution." Eaton. https://www.eaton.com/content/dam/eaton/markets/data-center/AC-Versus-DC-Power-Distribution.pdf (accessed 11/29/2020, 2020).
[12] T. Halder, "Comparative study of HVDC and HVAC for a bulk power transmission," in *International Conference on Power, Energy and Control (ICPEC)*, 2013, pp. 139-144.
[13] E. Planas, J. Andreu, J. I. Gárate, I. Martínez de Alegría, and E. Ibarra, "AC and DC technology in microgrids: A review," *Renewable and Sustainable Energy Reviews,* vol. 43, pp. 726-749, 2015.
[14] A. Kalair, N. Abas, and N. Khan, "Comparative study of HVAC and HVDC transmission systems," *Renewable and Sustainable Energy Reviews,* vol. 59, pp. 1653-1675, 2016.
[15] S. Qi, W. Sun, and Y. Wu, "Comparative analysis on different architectures of power supply system for data center and telecom center," in *IEEE International Telecommunications Energy Conference (INTELEC)*, 2017, pp. 26-29.
[16] B. R. Shrestha, U. Tamrakar, T. M. Hansen, B. P. Bhattarai, S. James, and R. Tonkoski, "Efficiency and Reliability Analyses of AC and 380 V DC Distribution in Data Centers," *IEEE Access,* vol. 6, pp. 63305-63315, 2018.
[17] M. Rivard, C. Fallaha, and J. Paquin, "Real-Time Simulation of a More Electric Aircraft Power Generation and Distribution System," in *AIAA/IEEE Electric Aircraft Technologies Symposium (EATS)*, 2018, pp. 1-10.
[18] S. Byahut and A. Uranga, "Power Distribution and Thermal Management Modeling for Electrified Aircraft," in *AIAA/IEEE Electric Aircraft Technologies Symposium (EATS)*, 2020, pp. 1-15.
[19] D. F. Finger, C. Braun, and C. Bil, "Case Studies in Initial Sizing for Hybrid-Electric General Aviation Aircraft," in *AIAA/IEEE Electric Aircraft Technologies Symposium (EATS)*, 2018, pp. 1-22.
[20] J. Chen, J. Shen, J. Chen, P. Shen, Q. Song, and C. Gong, "Investigation on the Selection and Design of Step-Up/Down 18-Pulse ATRUs for More Electric Aircrafts," *IEEE Transactions on Transportation Electrification,* vol. 5, no. 3, pp. 795-811, 2019.
[21] J. Sun, Z. Bing, and K. J. Karimi, "Small-signal modeling of multipulse rectifiers for more-electric aircraft applications," in *IEEE Power Electronics Specialists Conference*, 2008, pp. 302-308.
[22] S. M. Blair, C. D. Booth, I. M. Elders, N. K. Singh, G. M. Burt, and J. Mccarthy, "Superconducting fault current limiter application in a power-dense marine electrical system," *IET Electrical Systems in Transportation,* vol. 1, no. 3, pp. 93-102, 2011.
[23] S. Fletcher, P. Norman, S. Galloway, and G. Burt, "Solid state circuit breakers enabling optimised protection of DC aircraft power systems," in *Proceedings of the European Conference on Power Electronics and Applications*, 2011, pp. 1-10.